



# Crystal modulus of poly (lactic acid)s, and their stereocomplex

Lee, Sunglin  
Kimoto, Masayuki  
Tanaka, Masakazu  
Tsuji, Hideto  
Nishino, Takashi

---

## (Citation)

Polymer, 138:124-131

## (Issue Date)

2018-02-28

## (Resource Type)

journal article

## (Version)

Accepted Manuscript

## (Rights)

© 2018 Elsevier Ltd.

This manuscript version is made available under the CC-BY-NC-ND 4.0 license  
<http://creativecommons.org/licenses/by-nc-nd/4.0/>

## (URL)

<https://hdl.handle.net/20.500.14094/90004795>



# Crystal modulus of Poly (lactic acid)s, and their Stereocomplex

Sunglin LEE<sup>1</sup>, Masayuki KIMOTO<sup>1</sup>, Masakazu TANAKA<sup>1</sup>, Hideto TSUJI<sup>2</sup>, Takashi NISHINO<sup>1\*</sup>

<sup>1</sup>Department of Chemical Science and Engineering, Graduate School of Engineering, Kobe University, Rokko, Nada, Kobe 657-8501, Japan

<sup>2</sup>Department of Environmental and Life Sciences, Graduate School of Engineering, Toyohashi University of Technology, Tempaku-cho, Toyohashi 441-8580, Japan

## ABSTRACT

Elastic moduli of the crystalline regions (crystal modulus) of poly(lactic acid)s (PLA), poly (L-lactic acid) (PLLA), poly(D-lactic acid) (PDLA) and their stereocomplex (scPLA) in the directions parallel ( $E_l$ ) and perpendicular ( $E_t$ ) to the chain axis were measured by X-ray diffraction. The  $E_l$  value of PLLA and PDLA coincided as 14 GPa, whereas the  $E_l$  value of scPLA was 20 GPa at room temperature. These relatively low  $E_l$  values for PLAs and scPLA, compared with other polymers with planar zigzag skeletons in the crystalline regions, were considered to be attributed by helical structure. The difference of the  $E_l$  values between PLAs and scPLA could be explained by the difference of the helix types, that is,  $3_1$  helical skeleton of scPLA in the crystalline regions is slightly extended compared with  $10_3$  helix of PLAs. In addition, these  $E_l$  values were found to be temperature independent down to cryogenic temperature. The  $E_t$  values of scPLA were around 4 GPa, which is higher than those (around 3 GPa) of PLLA and PDLA. The higher melting point ( $\sim 230$  °C) compared with those ( $\sim 180$  °C) of PLLA and PDLA can be attributed to higher  $E_t$  value of scPLA, in other words, higher intermolecular interaction of scPLA compared with those of PLLA and PDLA. However, compared with the  $E_t$  value (4 GPa) of polyethylene where only van der Waals interaction acts, there exist no strong intermolecular interaction for PLAs and scPLA.

## KEYWORDS

## INTRODUCTION

Bio-based polymers are expected to be used as ecofriendly materials, to prevent environmental damage by mass-produced oil-based plastics. Among bio-based polymers, poly(lactic acid)(PLA,  $-(\text{CH}_2\text{CH}(\text{CH}_3)\text{COO})_n-$ ) is the most popular biodegradable aliphatic polyesters. PLA is synthesized by ring-opening polymerization of lactide, which is obtained by fermenting corn starch or sugar cane [1-3]. PLA has biocompatibility, hydrolyzability, and low emission of greenhouse gases. Therefore, PLA is very attractive for using not only in industrial fields, but also in biomedical applications, e.g., sutures, bone fixation, or drug delivery systems [4-9].

Ikada *et al.* discovered same amount of solution blend of poly(L-lactic acid) (PLLA) and poly(D-lactic acid) (PDLA) crystallized as stereocomplex in 1987 [10]. Since then, many procedures for making stereocomplex PLA (scPLA) from PLLA and PDLA, such as by solution blend, in a solid state blend from the melt, during polymerizations, were reported [11][12]. scPLA is known to show different structure and properties from PLAs. For example, scPLA shows higher melting point ( $\sim 230^\circ\text{C}$ ) than that ( $\sim 180^\circ\text{C}$ ) of PLAs. The unit cell of PLAs belongs to pseudo orthorhombic crystal system, which changes into triclinic system when stereocomplexation occurs [11]. PLLA and PDLA are reported to possess  $10_3$  helical conformation in the crystal lattice. On the contrary, scPLA possesses  $3_1$  helical conformation, similar to isotactic polypropylene (*it*.PP) [13].

The elastic modulus of the crystalline regions (crystal modulus) is one of the most important mechanical properties of polymers. The crystal moduli in the directions parallel ( $E_l$ ) and perpendicular ( $E_t$ ) to the chain axis have been measured by X-ray diffraction [14-17]. The data so far accumulated show the  $E_l$  value gives us information about the skeletal conformation, deformation mechanism, and maximum modulus for the specimen modulus of polymers. The  $E_l$  values for polymers with fully extended planar zigzag conformation, such as polyethylene (PE) is 235 GPa, whereas *it*.PP (helical structure) show the  $E_l$  value of 33 GPa. This

low  $E_t$  value of *it*.PP is due to that helical skeleton is easy to elongate to the stress direction compared with the planar zigzag one. On the other hand, the  $E_t$  values are correlated with the intermolecular interactions such as van der Waals force, dipole-dipole interaction, and hydrogen bonding, together with their anisotropies.

The crystal modulus of poly(L-lactic acid) (PLLA) was evaluated experimentally and theoretically [18][19]. However, we thought that only the crystal modulus of PLLA along the chain direction at room temperature is insufficient for overviewing the relationship between structure and properties of a series of PLA. For example, as mentioned above, the melting point of scPLA is more than 50 degree higher than those of PLLA and PDLA. However, as far as the authors know, no reasonable explanation on this phenomenon was described in the literatures. Intermolecular hydrogen bonding between CH<sub>3</sub> and C=O was proposed for PLLA by Ozaki *et al.* [20], but no information was available on the strength of intermolecular interaction of PLAs. In order to investigate these unsolved issues from the mechanical point of view, we decided to evaluate the crystal modulus of not only PLLA, but also those of PDLA and scPLA, including their crystal moduli both in the directions parallel and perpendicular to the chain axis. In addition, temperature dependence of the crystal modulus of PLLA, PDLA, and scPLA were also investigated in this study to examine the thermal properties of the crystalline regions of PLAs.

## EXPERIMENTAL SECTION

### *Samples*

PLLA pellets were kindly supplied from Unitika a Ltd. (4032DK), and PURASORB<sup>®</sup> for PDLA. Molecular weight of PLLA was  $4.5 \times 10^4$  for number average molecular weight ( $M_n$ ),  $9.5 \times 10^4$  for weight average molecular weight ( $M_w$ ). The  $M_n$ ,  $M_w$  of PDLA were  $1.1 \times 10^5$  and  $1.5 \times 10^5$ , respectively. The  $M_n$ ,  $M_w$  were measured by gel permeation chromatography using chloroform as an eluent, and polystyrene for molecular weight standards. The pellets were hot-pressed at 453 K, followed by slowly cooling to room

temperature. PLLA and PDLA film (thickness : 90  $\mu\text{m}$ ) was uniaxially drawn 6 times its original length at 348 K, then annealed at 408 K for 0.5 h at the constant length. In addition, highly oriented and highly crystallized PLLA by solid state extrusion (K-PLLA), kindly supplied from prof. T. Kanamoto in Science University of Tokyo, was also used for the crystal modulus measurement [21].

scPLA film was prepared by solution cast on glass petri dish, with the same weight ratio mixture of PLLA and PDLA dissolved in chloroform for each 1.5 wt%. Film was dried for 3 d at room temperature to remove solvent. Transparent film was successfully peeled off from the substrate. The film (thickness : 28  $\mu\text{m}$ ) was drawn 6 times its original length at 363 K, then annealed at 483 K for 1 h at the constant length.

### *Characterization*

The tensile properties of drawn and annealed PLLA, PDLA and scPLA films were measured at an extension rate of 2 mm/min with the initial length of 20 mm long using an Autograph AGS-1kND tensile tester (Shimadzu Co.,) at 300 K. The cross-section was prepared by cutting the film carefully with a glass knife normal to the sample surface. The cross-sectional area was evaluated from the density (1.24 g/cm<sup>3</sup> [22]), weight, and length of the sample. The means and standard deviations were evaluated for the macroscopic specimen modulus ( $Y_l$ ), tensile strength ( $\sigma_{max}$ ), and elongation at break ( $\epsilon_{max}$ ) measured for five samples.

The melting point ( $T_m$ ) and enthalpy of fusion ( $\Delta H$ ) of PLLA, PDLA and scPLA were measured using a differential scanning calorimeter (Rigaku Co., DSC 8230) with a sample weight of 3 mg, and a heating rate of 5 °C/min.  $T_m$  and  $\Delta H$  were determined as the peak temperature and area of the whole melting endotherm, respectively. Crystallinity  $X_c$  of PLLA, PDLA and scPLA were evaluated with the following equation (1).

$$X_c = \Delta H / \Delta H_0 \quad (1)$$

where  $\Delta H_0$  (PLLA and PDLA) = 93 J/g [23],  $\Delta H_0$  (scPLA) = 146 J/g [24], for 100 % crystallinity.

X-ray diffraction photographs were recorded on an imaging plate that had a camera length of 58 mm. The

specimen was irradiated perpendicular to the fiber axis with the  $\text{CuK}\alpha$  radiation generated by a Rigaku RINT-2000 operating at 40 kV and 20 mA.

To obtain the crystallite size  $D_{hkl}$ , the observed profiles for the  $(hkl)$  planes were corrected for the instrumental broadening according to the following equation (2).

$$\beta^2 = B^2 - b^2 \quad (2)$$

where  $\beta$  is the pure integral width of the reflection,  $B$  and  $b$  are the integral widths of the reflection for the drawn and annealed films and a standard sample, respectively. The correction for the doublet,  $\text{CuK}\alpha_1$  and  $\text{CuK}\alpha_2$ , broadening was calculated by the Jones method [25]. Finally,  $D_{hkl}$  were calculated using the Scherrer equation (3).

$$D_{hkl} = \lambda / \beta \cos \theta \quad (3)$$

where  $\theta$  is the Bragg angle of the reflections, and  $\lambda$  is the X-ray wavelength (1.5418 Å).

The degree of the crystallite orientation  $\pi$  was defined by the equation (4).

$$\pi = (180 - H^\circ) / 180 \quad (4)$$

where  $H^\circ$  is the half-width of the intensity distribution curve for the equatorial 200/110 reflection for PLLA, PDLA and 100/010/1-10 reflection for scPLA along the Debye-Scherrer ring.

#### *Elastic modulus of the crystalline regions*

The lattice extension under a constant load was measured by means of an X-ray diffractometer equipped with a stretching device and a load cell. The strain  $\varepsilon$  in the crystalline regions was estimated using the equation (5).

$$\varepsilon = \Delta d / d_0 \quad (5)$$

where  $d_0$  denotes the initial lattice spacing, and  $\Delta d$  is the change in lattice spacing induced by a constant stress. The experimental error in measuring the peak shift was evaluated ordinarily to be less than  $\pm 0.01^\circ$  at a  $2\theta$  angle.

The stress  $\sigma$  in the crystalline regions was assumed to be equal to the stress applied to the sample. This assumption of a homogeneous stress distribution has been proven experimentally for many polymers [26-28].

The crystal modulus  $E_l$  and  $E_t$  were calculated by the equation (6)

$$E_l = \sigma_l / \varepsilon_l, \quad E_t = \sigma_t / \varepsilon_t \quad (6)$$

where subscripts  $l$  and  $t$  mean the direction parallel and perpendicular to the chain axis, respectively.

The measurements have been described in more detail in our earlier publications [14-17, 26, 28-31].

Crystal modulus measurements at cryogenic temperature were performed with a cryogenic cell (Iwatani Industrial Gases Corp. Ministat CRT-006-7000) equipped apparatus constructed in our laboratory [29]. In these measurements, a stretching device and a load cell were combined with a cryostat cell and mounted on an X-ray goniometer. Helium gas was compressed and transported into the cold head attached to the top of the cryostat cell. Then, helium was adiabatically expanded, so the cold head was cooled to a cryogenic temperature of 13 K. The samples were clamped to the stretching device under a vacuum and cooled by thermal conduction via the clamp connected to the cold head. Full details are described elsewhere [30][31].

## RESULTS AND DISCUSSION

### *Sample Characteristics*

Figure 1 shows X-ray fiber photographs of drawn and annealed PLLA, PDLA and scPLA film at 300 K. All samples were highly crystallized and the crystallites were highly oriented along the drawn direction.

The fiber photographs of PLLA and PDLA were that of typical  $\alpha$ -form, which were completely different from that of scPLA. We confirmed the scPLA film contained only scPLA, as no more PLLA and PDLA peak appeared on the fiber photograph. From the fiber photograph and meridional X-ray diffraction profile (Figure S1), K-PLLA possessed extremely high crystallite orientation, crystallinity, low lattice disorder, and  $\alpha$ -form was only appeared, too.

Figure 2 shows (upper) meridional and (lower) equatorial X-ray diffraction profiles of drawn and annealed PLLA, PDLA and scPLA film at 300 K. On the basis of the reported crystal lattice of PLLA and PDLA (orthorhombic,  $a = 10.6 \text{ \AA}$ ,  $b = 6.1 \text{ \AA}$ ,  $c$  (fiber axis)  $= 28.8 \text{ \AA}$ ) [32] and scPLA (triclinic,  $a = 9.16 \text{ \AA}$ ,  $b = 9.16 \text{ \AA}$ ,  $c$  (fiber axis)  $= 8.7 \text{ \AA}$ ,  $\alpha, \beta = 109.2^\circ$ ,  $\gamma = 109.8^\circ$ ) [13], the diffraction peaks could be indexed as shown in the figure, respectively. Meridional 0010 reflection for PLLA and PDLA, -2-26 reflection for scPLA were used to measure the  $E_l$  values. The normal of the -2-26 reflection is inclined at an angle of  $1.3^\circ$  from the meridian. This angle coincides with the angle expected from the crystal structure. Therefore, in fact for crystal modulus measurement, the inclination correction should be needed. However,  $\sigma$  and  $\varepsilon$  were not corrected for the inclination of this lattice plane, because it is negligibly small [33]. The  $E_l$  values were measured for 200/110 and 020 reflections for PLLA and PDLA, 100/010/1-10, 110/-120/-210, 200/020/2-20 reflections for scPLA, respectively.

Table 1 summarized sample preparation conditions (drawing, annealing), and characteristics (crystallite orientation, crystallinity, crystallite size, melting point  $T_m$ , Young's modulus  $Y_l$ , tensile strength  $\sigma_{max}$  and elongation at the break  $\varepsilon_{max}$ ) of PLLA, PDLA and scPLA. (Table S1 summarized the equatorial crystallite sizes of PLLA, PDLA and scPLA) Though PDLA showed a little bit larger crystallite size and higher melting point, PLLA and PDLA intrinsically showed same properties. Compared with PLAs, scPLA showed low crystallinity and small crystallite size, but it possessed higher mechanical properties and higher melting point (approximately  $40^\circ\text{C}$ ).



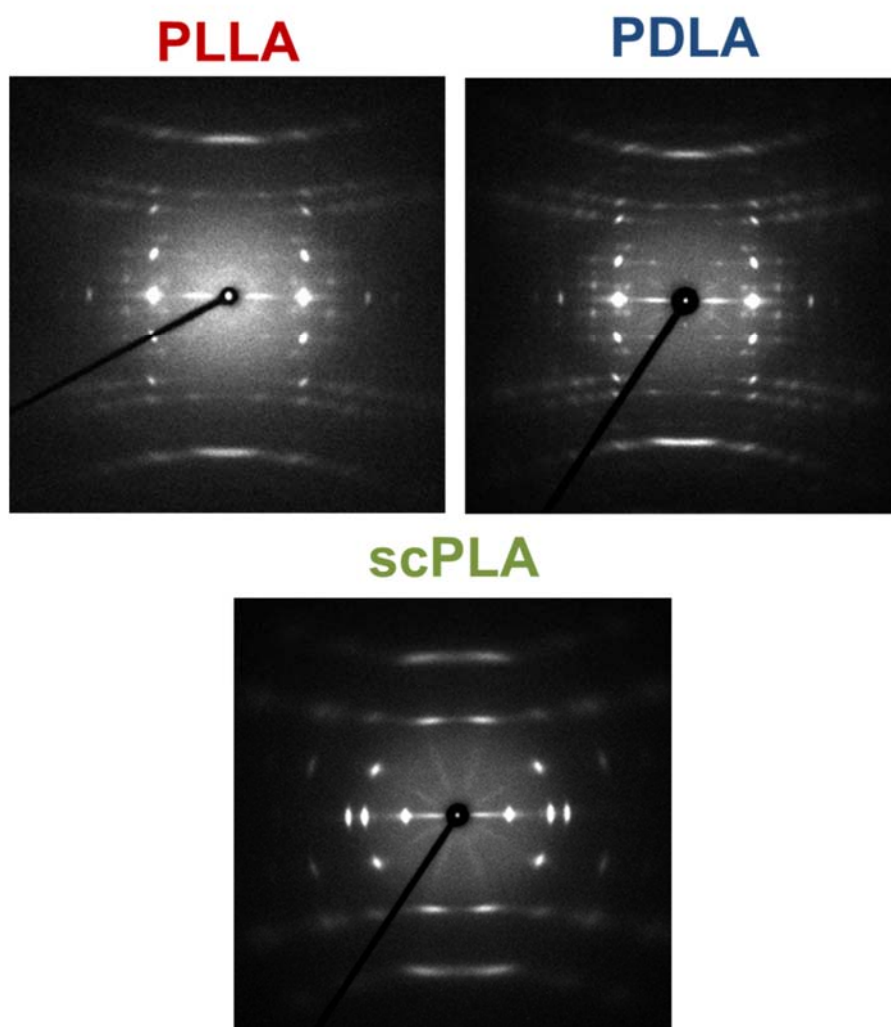


Fig 1. X-ray fiber photographs of PLLA, PDLA and scPLA.

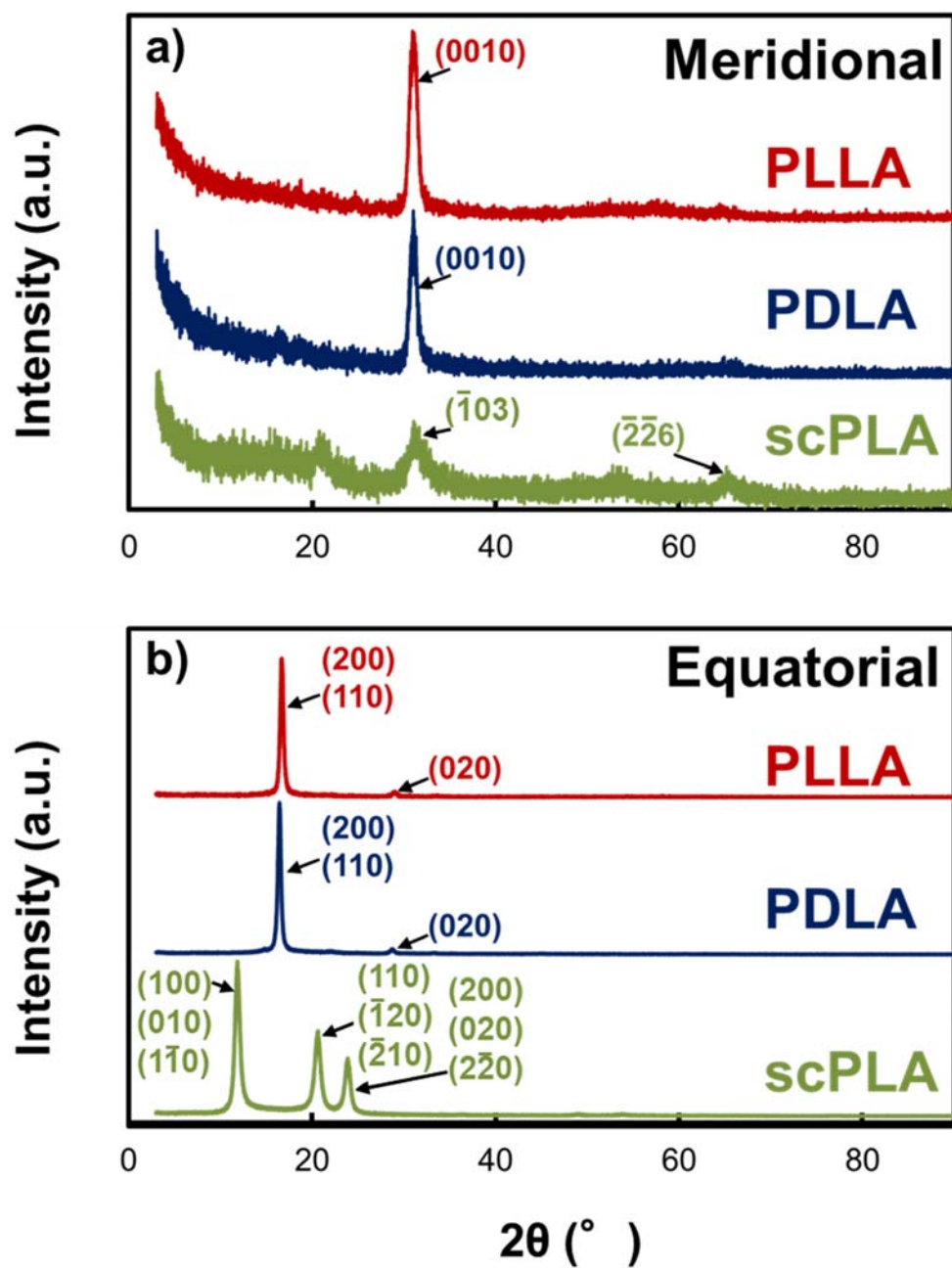


Fig. 2 a) Meridional and b) equatorial X-ray diffraction profiles of PLLA, PDLA and scPLA.

Table 1 Sample preparation conditions (drawing, annealing), crystallite orientation, crystallinity, crystallite size, melting point  $T_m$ , Young's modulus  $Y_l$ , tensile strength  $\sigma_{max}$  and elongation at the break  $\epsilon_{max}$  of PLLA, PDLA and scPLA.

	PLLA	PDLA	scPLA
Drawing	$\lambda = 6$ @75 °C		$\lambda = 6$ @90 °C
Annealing	@ 135 °C 0.5 h		@ 210 °C 1 h
Crystallite orientation	0.97	0.96	0.95
Crystallinity (%)	61	68	36
Crystallite size (Å)			
(0010)	88	104	—
(-2-26)	—	—	57
$T_m$ (°C)	165.3	180.9	214.1
$Y_l$ (GPa)	6.2	5.8	5.6
$\sigma_{max}$ (MPa)	128	179	108
$\epsilon_{max}$ (%)	43	48	19

### Crystal modulus $E_l$

Figure 3 shows the stress  $\sigma$ -strain  $\epsilon$  curves for the 0010 reflections of ( $\circ$ ) PLLA and ( $\square$ ) PDLA together with that ( $\blacktriangle$ ) of K-PLLA at 300 K. All the plots could be expressed with a straight line with the same inclination through the origin, and the lattice extensions were always reversible. The initial inclination of this line gave the crystal modulus  $E_l$  of PLLA, PDLA and K-PLLA as 14 GPa at 300 K. Same crystal modulus  $E_l$  for PLLA, PDLA and K-PLLA even with different microstructures supports the homogeneous stress distribution. As mentioned previously, the crystal modulus corresponds to the maximum modulus, because the elastic modulus were measured by X-ray diffraction method where only the polymer crystallite were detected. Pennings *et al.* attempted to get high modulus / high strength fiber using PLLA [5]. They succeeded to increase strength up to 1 GPa, but the modulus remained low (<10 GPa). A lot has been tried for getting high modulus PLLA fiber, but failed [34][35]. As mentioned above, the reason for low macroscopic modulus of PLLA fiber can be attributed to low crystal modulus of PLLA, and so called high modulus fiber/film can not be obtained using PLLA and PDLA. In addition, PLLA is often applied in biomedical fields [8][9], but low crystal modulus also suggests that PLLA alone is not suitable for bone replacement, and some reinforcement will be needed for this purpose.

The observed  $E_l$  values (14 GPa) of PLAs are much lower than that (235 GPa) of PE with a fully extended planar zigzag conformation in the crystalline regions. If the PLA skeleton is assumed to be fully extended planar zigzag, the  $E_l$  value, evaluated by Treloar's method [36][37] using the reported bond lengths, bond angles and these force constants (see Table S2), was 120 GPa, which is 8.6 times higher compared with the observed one.

De Oca *et al.*[18] calculated the crystal modulus of PLLA  $\alpha$ -form, as 36 GPa, based on the lattice model proposed by Kobayashi *et al.*[38], in which two  $10_3$  helices are packed in the unit cell. However, Tashiro *et al.*[19] suggest their modulus calculation cannot be assumed to be satisfactorily exact since the crystal structure employed by them is not enough reasonable. On the contrary, Tashiro *et al.* calculated the  $E_l$  value

for  $10_3$  helical  $\alpha$ -form on the basis of the refined crystal structures of PLLA as 14.7 GPa. They also observed the  $E_l$  value for PLLA  $\alpha$ -form as 13.76 GPa, which coincided with the  $E_l$  value in this study. We here confirmed the linearity of  $\sigma$ - $\epsilon$  curve up to higher  $\sigma$  both for PLLA, PDLA (Figure 3) with wide variety of microstructure, compared with the previous one ( $\sigma < 60$  MPa)[19]. This supports higher reliability of the results in the present study.

As mentioned in introduction, helical skeleton gives low  $E_l$  value than that of planar zigzag one. The contraction of  $10_3$  helical structure is calculated as approximately 20 % from planar zigzag conformation in the crystalline regions [39]. The bigger contraction brings the smaller the  $E_l$  value. Therefore, the low  $E_l$  value of PLLA and PDLA will be explained by helical skeleton in the crystalline regions.

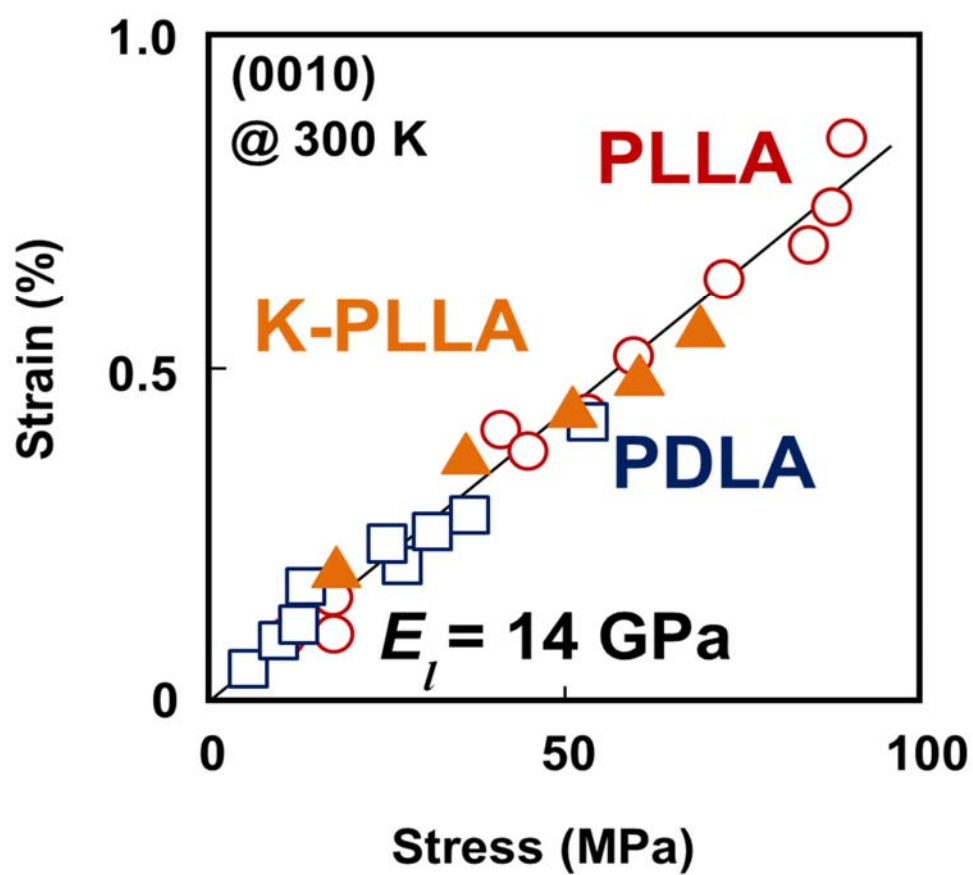


Fig. 3 Stress-strain curves for the (0010) plane of (○) PLLA, (□) PDLA and (▲) K-PLLA at 300K.

Figure 4 show the  $\sigma$ - $\epsilon$  curve for the  $\bar{2}\bar{2}6$  reflections of scPLA, together with the results of Fig.3 expressed with the dotted line, at 300 K. All the plots could be expressed with a straight line with the same inclination through the origin, and the lattice extensions were always reversible. The initial inclination of the line gave the crystal modulus  $E_l$  of scPLA as 20 GPa at 300 K. This is higher as 140 % compared with those of PLLA and PDLA. Okihara *et al.*[13] proposed the crystal structure of scPLA, as  $3_1$  helical conformation. This slightly extended conformation ( $3_1$  helix) brings scPLA become hard to extend (elongation) characteristic to scPLA skeleton. Therefore,  $3_1$  helix (scPLA) shows higher  $E_l$  value compared with that  $10_3$  helix (PLLA and PDLA).

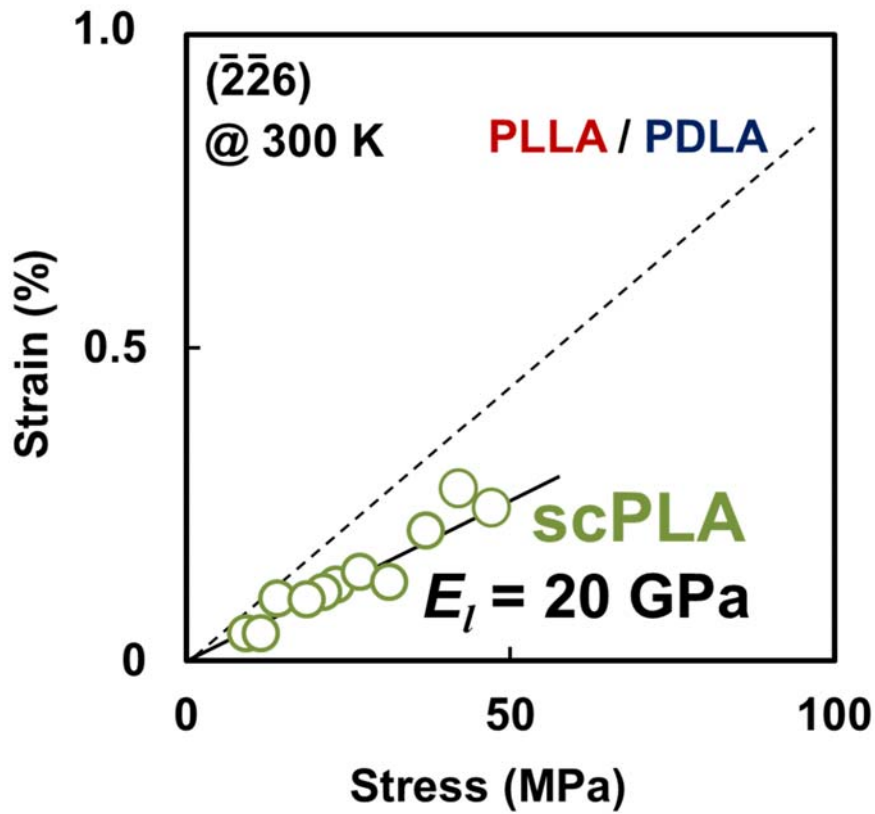


Fig. 4 Stress-strain curves for the (○) ( $\bar{2}\bar{2}6$ ) plane of scPLA at 300K. Broken line represent the results in Fig.3 for comparison.

Figure 5 shows the relationship between temperature and the crystal modulus  $E_l$  for the (0010) plane of (○) PLLA, (□) PDLA and (-2-26) plane of (○) scPLA. (Figure S2 shows the stress–strain curves for the (0010) plane of (○) PLLA and (□) PDLA, (-2-26) plane of (○) scPLA at various temperature. The  $E_l$  values were evaluated from the initial inclination of each curve at each temperature.) The  $E_l$  values of PLLA and PDLA was 14 GPa at 13 K, which is the same at room temperature. For scPLA, the  $E_l$  value was 22 GPa at 13 K, which is slight higher than that at room temperature. However, the  $E_l$  value of scPLA at cryogenic temperature can be said to be almost same as that of room temperature, considering the experimental error ( $\pm 10\%$ ). So it is suggested that PLAs and their stereocomplex are stable against the heat. These are in the contrast with the results for PGA, where the  $E_l$  value of PGA show temperature dependence from cryogenic

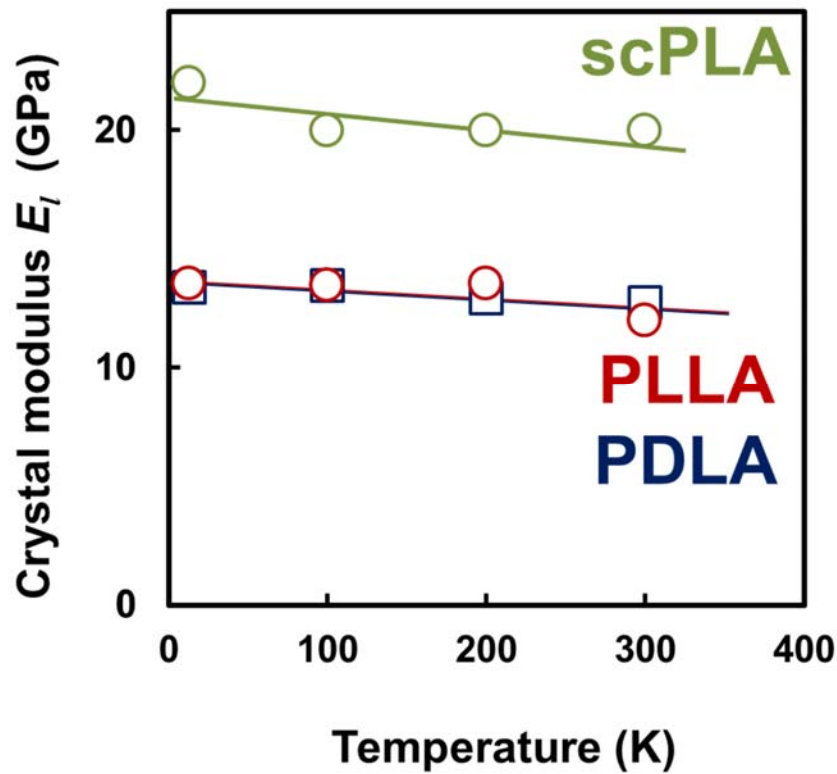


Fig.5 Relationship between temperature and crystal modulus  $E_l$  for the (0010) plane of (○) PLLA, (□) PDLA and (○) ( $\bar{2}\bar{2}6$ ) plane of scPLA.

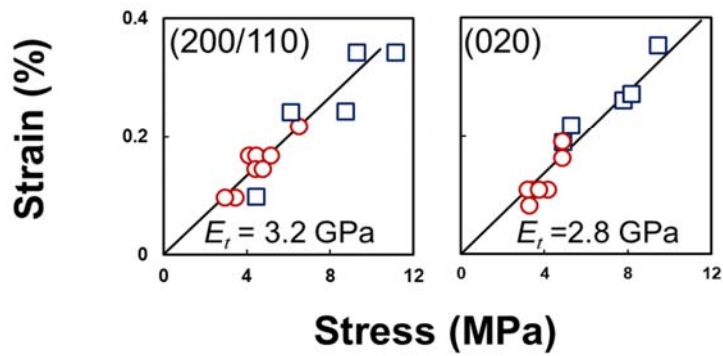


temperature to high temperature [28]. Even same C-O-C repeated unit in molecular chain, the difference between PLAs and PGA is due to that helical skeleton of PLAs is already largely contracted in the crystalline regions, and their structural effect surpasses the temperature effect.

#### *Crystal modulus $E_t$*

Figure 6 show the stress  $\sigma$  - strain  $\epsilon$  curves for the equatorial (200/110), (020) planes of ( $\circ$ ) PLLA, ( $\square$ ) PDLA and (100/010/1-10), (110/-120/-210), (200/020/2-20) planes of scPLA at 300 K, respectively. The curves for the equatorial reflections could be also expressed with a straight line through the origin, and the lattice extensions were always reversible. The  $E_t$  values of PLLA and PDLA were 3.2 and 2.8 GPa for the (200/110) and (020) planes, respectively, at 300 K. These  $E_t$  values are smaller than that (4 GPa) of PE only based on van der Waals intermolecular interaction [26] or that (6.6 GPa) of poly(vinyl alcohol) (PVA) based on intermolecular hydrogen bonds [17]. Thus, these results suggest van der Waals intermolecular interactions mainly act in PLLA and PDLA molecules in the crystal lattice. On the other hands, the  $E_t$  values of scPLA were 4.0, 4.6 and 4.1 GPa for (100/010/1-10), (110/-120/-210) and (200/020/2-20) planes at 300 K, respectively. These  $E_t$  values of scPLA are higher than those of PLLA and PDLA. These reveal scPLA possesses higher intermolecular cohesive energy compared with PLAs. Ozaki *et al.* [20] suggest there are hydrogen bonds of  $\text{CH}_3 \cdots \text{O}=\text{C}$ , in the stereocomplex crystals. However, judging from the  $E_t$  values of scPLA (just same as PE, also much smaller than those of PVA or polyamides which possess hydrogen bonds), no strong hydrogen bonding acts from the mechanical point of view.

## PLLA / PDLA



## scPLA

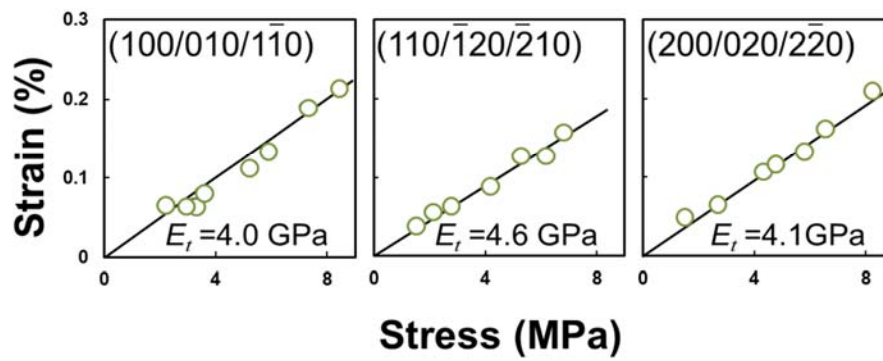


Fig.6 Stress-strain curves for the equatorial planes of PLLA, PDLA and scPLA at 300 K.

Figure 7 shows anisotropy of the  $E_t$  value superimposed with the molecular packing in the  $ab$  plane of PLLA and PDLA at 300 K [13]. The anisotropies of the  $E_t$  values in PLLA and PDLA were calculated from the observed  $E_t$  values using following equation (7) [40].

$$\frac{1}{E_\theta} = \frac{\cos^4\theta}{E_0} + \frac{\sin^4\theta}{E_{90}} + \left[ \frac{1}{G_{0,90}} - 2 \left( \frac{\nu_{0,90}}{E_0} \right) \right] \sin^4\theta * \cos^4\theta \quad (7)$$

where  $E_\theta$  is the  $E_t$  value at the angle of  $\theta$  from a-axis,  $E_0$  and  $E_{90}$  are  $E_t$  value along a- and b-axis,  $G_{0,90}$  is shear modulus in a- and b- axis direction.  $\nu_{0,90}$ , Poisson's ratio was assumed to be 0.33 in the present study.

The  $E_t$  values are almost isotropic for PLLA and PDLA, and no difference between PLLA and PDLA even these possess opposite helical direction, respectively. Wasanasuk and Tashiro [19] calculated the  $E_t$  values of PLA, and reported that they were almost comparable to that of PE, *it*.PP, but far below compared with those of PVA, Nylon6. In addition, calculated  $E_t$  value was almost isotropic in the  $ab$  plane. These calculation also coincide with the observed ones in Figure 7,8.

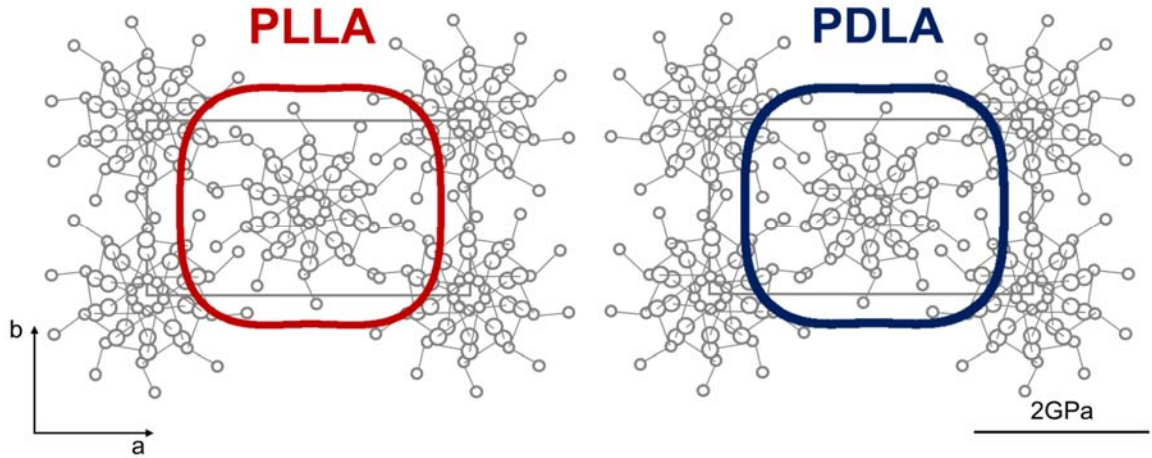


Fig.7 Anisotropies of the  $E_t$  values in the  $ab$  plane of PLLA and PDLA at 300K.

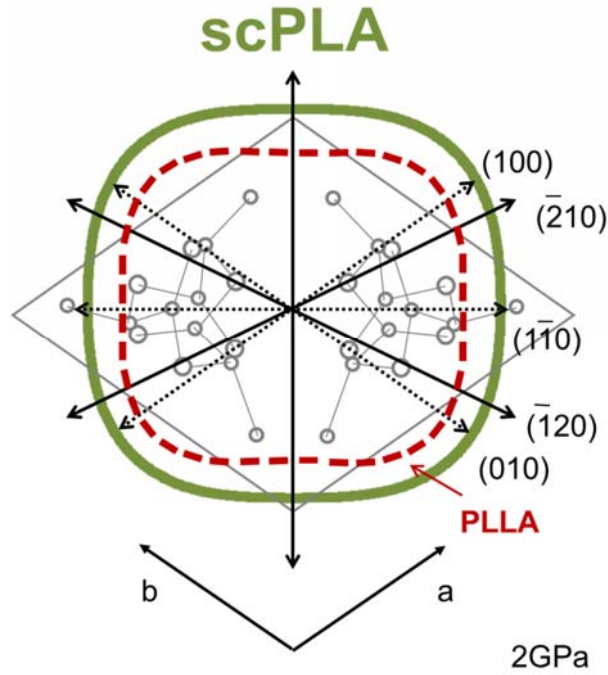


Fig.8 Anisotropy of the  $E_t$  value in the  $ab$  plane of scPLA at 300K. The results in Fig.7 is superimposed with (-) the dotted line at 300K.

Figure 8 shows anisotropy of the  $E_t$  values and the molecular packing of scPLA in the  $ab$  plane at 300 K [41], together with that of PLLA with the dotted line for comparison. The unit cell contains one PLLA and one PDLA chain with shape of an equilateral triangle, and reported to be formed equilateral-triangle-shaped single crystals of the scPLA [13][42]. The arrows express the  $E_t$  value corresponding to each directions. The  $E_t$  values of scPLA are almost isotropic as same trend as those of PLLA and PDLA [19]. However, compared with PLLA and PDLA, scPLA possess higher  $E_t$  values for all directions. These results indicate there are stronger intermolecular interaction between PLLA and PDLA molecular chains, compared in the cases between PLLA/PLLA, PDLA/PDLA combinations.

The melting point is defined as the ratio of the change in entropy of fusion ( $\Delta S$ ) and enthalpy of fusion ( $\Delta H$ ), ( $T_m = \Delta H/\Delta S$ ). As discussed in the previous paper [28], the  $E_t$  values can be correlated with  $\Delta H$  from mechanical point of view. The higher melting point ( $\sim 230^\circ\text{C}$ ) compared with those ( $\sim 180^\circ\text{C}$ ) of PLLA and PDLA can be attributed to higher  $E_t$  value of scPLA, in other words, higher intermolecular interaction of scPLA compared with those of PLLA and PDLA.

## CONCLUSIONS

Crystal moduli of PLLA, PDLA and scPLA in the directions both parallel ( $E_l$ ) and perpendicular ( $E_t$ ) to the chain axis were measured by X-ray diffraction. PLLA and PDLA possess same  $E_l$  value as 14 GPa, even though, they possess opposite chain helical direction, at room temperature. This small  $E_l$  value is caused by largely contracted  $10_3$  helical structure in the crystalline regions for PLLA and PDLA. The  $E_l$  value of scPLA is 20 GPa at room temperature, being higher than those of PLLA and PDLA. This is due to that the skeleton of scPLA is slightly extended ( $3_1$  helix) than those of PLLA and PDLA. All PLLA, PDLA and scPLA showed temperature independence of the  $E_l$  values from cryogenic temperature to room temperature, which is considered that the structural effect on the  $E_l$  value is higher than the temperature effect. Even with the existence/ absence of methyl groups inserted on the side chain, the results of PLA was quite different from those of PGA [28]. The  $E_t$  values of PLLA and PDLA were smaller than that of PE. These suggest that only weak van der Waals intermolecular interactions act in PLLA and PDLA. The  $E_t$  value of scPLA was slightly higher than those of PE, PLLA and PDLA, however, they were lower than that based on hydrogen bonding.

## ASSOCIATED CONTENT

### Supporting Information

Figure S1, S2 and Table S1, S2.

## AUTHOR INFORMATION

### Corresponding Authors

\*E-mail: tnishino@kobe-u.ac.jp

## ACKNOWLEDGMENTS

Solid state extruded PLLA sample was kindly supplied from Professors Tetsuo Kanamoto (Science University of Tokyo). This work was supported by the Special Coordination Fund for the Promotion of Science and Technology, Creation of Innovation Centers for Advanced Interdisciplinary Research Areas (Innovative Bioproduction Kobe), MEXT, Japan.

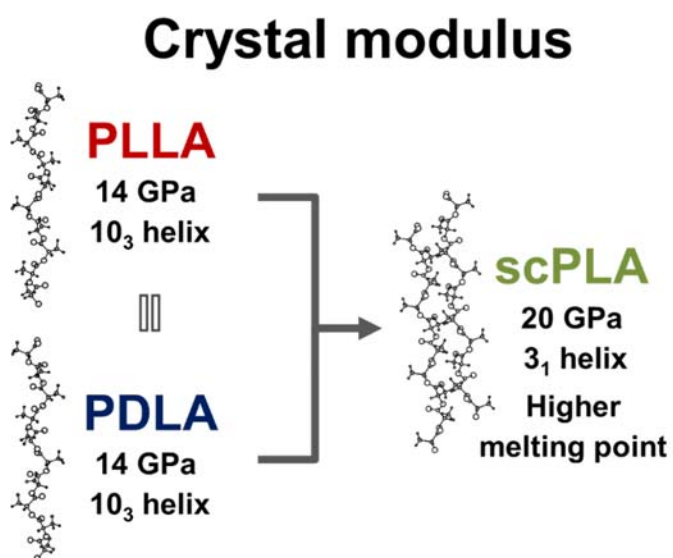
## REFERENCES

- [1] H. Tsuji, Hydrolytic Degradation, in: R. Auras, L.-T. Lim, S.E.M. Selke, H. Tsuji (Eds.), *Poly(Lactic Acid)*, John Wiley & Sons, Inc., Hoboken, NJ, USA, 2010: pp. 343–381.
- [2] Y. Ikada, H. Tsuji, Biodegradable polyesters for medical and ecological applications, *Macromol. Rapid Commun.* 21 (2000) 117–132.
- [3] H. Tsuji, Y. Ikada, Properties and morphologies of poly(L-lactide): 1. Annealing condition effects on properties and morphologies of poly(L-lactide), *Polymer* 36 (1995) 2709–2716.
- [4] H. Tsuji, S. Noda, T. Kimura, T. Sobue, Y. Arakawa, Configurational Molecular Glue: One Optically Active Polymer Attracts Two Oppositely Configured Optically Active Polymers, *Sci. Rep.* 7 (2017) 45170.
- [5] B. Eling, S. Gogolewski, A.J. Pennings, Biodegradable materials of poly(l-lactic acid): 1. Melt-spun and solution-spun fibres, *Polymer* 23 (1982) 1587–1593.
- [6] S. Gogolewski, A.J. Pennings, Resorbable materials of poly(L-lactide). II. Fibers spun from solutions of poly(L-lactide) in good solvents, *J. Appl. Polym. Sci.* 28 (1983) 1045–1061.
- [7] J.W. Leenslag, S. Gogolewski, A.J. Pennings, Resorbable materials of poly(L-lactide). V. Influence of secondary structure on the mechanical properties and hydrolyzability of poly(L-lactide) fibers produced by a dry-spinning method, *J. Appl. Polym. Sci.* 29 (1984) 2829–2842.
- [8] K.A. Athanasiou, G.G. Niederauer, C.M. Agrawal, Sterilization, toxicity, biocompatibility and clinical applications of polylactic acid/polyglycolic acid copolymers, *Biomaterials* 17 (1996) 93–102.
- [9] A.S. Hoffman, Hydrogels for biomedical applications, *Adv. Drug Deliv. Rev.* 64 (2012) 18–23.
- [10] Y. Ikada, K. Jamshidi, H. Tsuji, S.H. Hyon, Stereocomplex Formation between Enantiomeric Poly(lactides), *Macromolecules* 20 (1987) 904–906.

- [11] H. Tsuji, Poly(lactide) stereocomplexes: Formation, structure, properties, degradation, and applications, *Macromol. Biosci.* 5 (2005) 569–597.
- [12] H. Tsuji, Poly ( lactic acid ) stereocomplexes : A decade of progress, *Adv. Drug Deliv. Rev.* 107 (2016) 97–135.
- [13] T. Okihara, M. Tsuji, A. Kawaguchi, I. Katayama, H. Tsuji, S. Hyon, Y. Ikada, Crystal structure of stereocomplex of poly ( L- lactide ) and poly ( D-lactide ), *J. Macromol. Sci. Part B.* 30 (1991) 119–140.
- [14] T. Nishino, R. Matsui, K. Nakamae, Elastic modulus of the crystalline regions of chitin and chitosan, *J. Polym. Sci. Part B Polym. Phys.* 37 (1999) 1191–1196.
- [15] K. Nakamae, T. Nishino, Y. Shimizu, T. Matsumoto, Experimental Determination of the Elastic Modulus of Crystalline Regions of Some Aromatic Polyamides, Aromatic Polyesters, and Aromatic Polyether Ketone, *Polym. J.* 19 (1987) 451–459.
- [16] T. Nishino, K. Tada, K. Nakamae, Elastic modulus of crystalline regions of poly(ether ether ketone), poly(ether ketone) and poly(p-phenylene sulphide), *Polymer* 33 (1992) 736–743.
- [17] K. Nakamae, T. Nishino, H. Ohkubo, S. Matsuzawa, K. Yamaura, Studies on the temperature dependence of the elastic modulus of crystalline regions of polymers: 14. Poly(vinyl alcohol) with different tacticities, *Polymer* 33 (1992) 2581–2586.
- [18] H.M. de Oca, I.M. Ward, Structure and mechanical properties of poly(L-lactic acid) crystals and fibers, *J. Polym. Sci. Part B Polym. Phys.* 45 (2007) 892–902.
- [19] K. Wasanasuk, K. Tashiro, Theoretical and experimental evaluation of crystallite moduli of various crystalline forms of poly(l -lactic acid), *Macromolecules* 45 (2012) 7019–7026.
- [20] J. Zhang, Y. Duan, H. Sato, H. Tsuji, I. Noda, S. Yan, Y. Ozaki, Crystal modifications and thermal behavior of poly(L-lactic acid) revealed by infrared spectroscopy, *Macromolecules* 38 (2005) 8012–8021.
- [21] D. Sawai, K. Takahashi, A. Sasashige, T. Kanamoto, S.-H. Hyon, Preparation of Oriented  $\beta$ -Form Poly(L-lactic acid) by Solid-State Coextrusion: Effect of Extrusion Variables, *Macromolecules* 36 (2003) 3601–3605.
- [22] D.E. Henton, P. Gruber, J. Lunt, J. Randall, Chapter 16. Polylactic Acid Technology, *Nat. Fibers, Biopolym. Biocomposites* (2005) 527–578.
- [23] E.W. Fischer, H.J. Sterzel, G. Wegner, Investigation of the structure of solution grown crystals of lactide copolymers by means of chemical reactions, *Kolloid-Z. U. Z. Polym.* 251 (1973) 980–990.
- [24] H. Tsuji, Y. Ikada, F. Horii, M. Nakagawa, H. Odani, R. Kitamaru, Stereocomplex Formation between Enantiomeric Poly(lactic acid)s. 7. Phase Structure of the Stereocomplex Crystallized from a Dilute Acetonitrile Solution As Studied by High-Resolution Solid-State  $^{13}\text{C}$  NMR Spectroscopy, *Macromolecules* 25 (1992) 4114–4118.
- [25] F.W. Jones, The Measurement of Particle Size by the X-Ray Method, *Proc. R. Soc. A Math. Phys. Eng. Sci.* 166 (1938) 16–43.

- [26] K. Nakamae, T. Nishino, H. Ohkubo, Elastic modulus of crystalline regions of polyethylene with different microstructures: Experimental proof of homogeneous stress distribution, *J. Macromol. Sci. Part B.* 30 (1991) 1–23..
- [27] I. Sakurada, T. Ito, K. Nakamae, Elastic moduli of polymer crystals for the chain axial direction, *Makromol. Chem.* 75 (1964) 1–10.
- [28] S. Lee, C. Hongo, T. Nishino, Crystal Modulus of Poly(glycolic acid) and Its Temperature Dependence, *Macromolecules* 50 (2017) 5074–5079.
- [29] T. Nishino, H. Miyazaki, K. Nakamae, X-ray diffraction of polymer under load at cryogenic temperature, *Rev. Sci. Instrum.* 73 (2002) 1809.
- [30] T. Nishino, T. Okamoto, H. Sakurai, Cryogenic mechanical behavior of poly(trimethylene terephthalate), *Macromolecules* 44 (2011) 2106–2111.
- [31] M. Kotera, A. Nakai, M. Saito, T. Izu, T. Nishino, Elastic Modulus of the Crystalline Regions of Poly (p-phenylene terephthalamide) Single Fiber Using SPring-8 Synchrotron Radiation, *Polym. J.* 39 (2007) 1295–1299.
- [32] W. Hoogsteen, A. Postema, Crystal structure, conformation and morphology of solution-spun poly (L-lactide) fibers, *Macromolecules* 23 (1990) 634–642.
- [33] K. Nakamae, T. Nishino, F. Yokoyama, T. Matsumoto, Temperature dependence of the elastic modulus of crystalline regions of Poly(ethylene terephthalate), *J. Macromol. Sci. Part B.* 27 (1988) 407–420.
- [34] R. Inai, M. Kotaki, S. Ramakrishna, Structure and properties of electrospun PLLA single nanofibres, *Nanotechnology* 16 (2005) 208–213.
- [35] K. Mezghani, J.E. Spruiell, High speed melt spinning of poly(L-lactic acid) filaments, *J. Polym. Sci. Part B Polym. Phys.* 36 (1998) 1005–1012.
- [36] L.R.G. Treloar, Calculations of elastic moduli of polymer crystals: II. Terylene, *Polymer* 1 (1960) 279–289.
- [37] L.R.G. Treloar, Calculations of elastic moduli of polymer crystals: 1. Polyethylene and Nylon 66, *Polymer* 1 (1959) 95–103.
- [38] J. Kobayashi, T. Asahi, M. Ichiki, A. Oikawa, H. Suzuki, T. Watanabe, E. Fukada, Y. Shikunami, Structural and optical properties of poly lactic acids, *J. Appl. Phys.* 77 (1995) 2957–2973.
- [39] K. Nakamae, T. Nishino, S. Takagi, Temperature dependence of the elastic modulus of crystalline regions of isotactic poly(4-methyl-1-pentene), *J. Macromol. Sci. Part B.* 30 (1991) 47–62.
- [40] J.F. Ney, *Physical Properties of Crystals*; Oxford at the Clarendon Press, Oxford, U.K., 1957
- [41] D. Brizzolara, H.J. Cantow, K. Diederichs, E. Keller, a J. Domb, Mechanism of the stereocomplex formation between enantiomeric poly(lactide)s, *Macromolecules* 29 (1996) 191–197.
- [42] F. Zhang, H.W. Wang, K. Tominaga, M. Hayashi, S. Lee, T. Nishino, Elucidation of Chiral Symmetry Breaking in a





Graphical Abstracts